An Introduction to the Volume Conjecture

by
Dylan O'Connor

Senior Honors Thesis
Mathematics
University of North Carolina at Chapel Hill

April 28, 2020

Approved:

David Rose, Thesis Advisor
Richard Rimanyi, Reader
Lev Rozansky, Reader

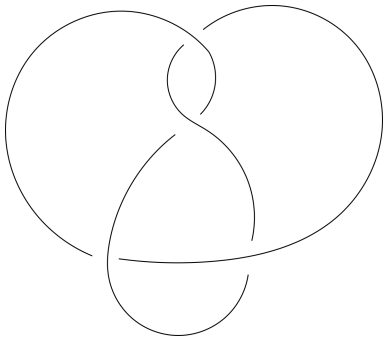

Figure 1: A figure-8 knot diagram

1 Introduction

In this thesis we discuss the volume conjecture and explicitly develop the necessary background in knot theory and hyperbolic geometry to understand its statement. First, we will provide some context.

The main objects we will study in this paper are knots.

Definition 1. *A **knot** is a smooth embedding of $\mathbb{S}^1$ into $\mathbb{S}^3$.*

We will also need to consider links, which are closely related to knots:

Definition 2. *An n-component **link** is a smooth embedding of n copies of $\mathbb{S}^1$ into $\mathbb{S}^3$.*

We often study knots and links by knot (or link) diagrams, which are generic projections of knots into two dimensions, that is, projections which keep crossing information, require that only two strands cross at any one point, do not allow tangencies, and have only transverse crossings. A knot diagram for the figure eight knot is given in figure 1. Unfortunately, multiple diagrams can represent the same knot, and it is not always easy to tell whether two given diagrams represent the same knot.

Definition 3. *A **knot (or link) invariant** is a function of equivalence classes of knots under the equivalence relation of ambient isotopy, or an orientation preserving homeomorphism of $\mathbb{S}^3$ to itself which takes one knot or link to another.*

We frequently use knot diagrams to find invariants, as we will see in the next section. The volume conjecture concerns two very different kinds of knot invariant. Thurston proved the following theorem:

Theorem 1. *(Thurston) Every knot is either a hyperbolic knot, a torus knot, or a satellite knot.*

Definition 4. *A **torus knot** is a knot which lies on a torus. Roughly speaking, a **satellite knot** is a knot built on the structure of a simpler knot. Finally, a*

hyperbolic *knot is a knot whose complement in* $\mathbb{S}^3$ *admits a complete hyperbolic structure.*

Thanks to their relatively strict structures, torus knots are relatively well-understood compared to hyperbolic knots. Meanwhile, satellite knots can in some sense be generated from either torus or hyperbolic knots, so understanding hyperbolic knots better will bring us closer to an understanding of knots in general. It turns out that in the hyperbolic metric, the volumes of hyperbolic knot complements are finite. Thus, Mostow's rigidity theorem applies to them. The statement of the theorem (for our purposes, anyway) follows:

Theorem 2. *(Mostow) Suppose* M *is a finite-volume 3-manifold. If* M *has a complete hyperbolic metric, then it is the only complete hyperbolic metric on* M *up to isometry.*

This means that the complete hyperbolic structure on a knot complement is a knot invariant. (Since the knot complement is a property of the 3-dimensional knot, it does not depend on a knot or link diagram.) Accordingly, anything we calculate using that metric, like the volume of the knot complement, for example, is also an invariant. These invariants all depend only on geometry.

On the other hand, Jones discovered a link invariant calculable by purely algebraic means called the Jones polynomial. Amazingly, the volume conjecture directly relates a generalization of the Jones polynomial, the colored Jones polynomial, to the volume of the knot complement. Here is the statement of the conjecture:

Conjecture 1.

$$\lim_{N\to\infty} \frac{2\pi \log|J_N(K; e^{\frac{\pi i}{N}})|}{N} = \mathrm{Vol}(K)$$

for all hyperbolic knots K*, where* $\mathrm{Vol}(K)$ *is the volume of* $\mathbb{S}^3 \setminus K$*, and where* $J_N(K; e^{\frac{\pi i}{N}})$ *is the* N*-th colored Jones polynomial of* K *evaluated at* $e^{\frac{\pi i}{N}}$*.*

2 Jones Polynomial

Reidemeister discovered an important tool for developing link invariants.

Definition 5. *The following three local operations on knot diagrams are known as the* ***Reidemeister moves***

RI:

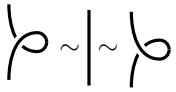

RII:

RIII:

Reidemeister also proved the following theorem, which we will not prove here.

Theorem 3. *Two knot (or link) diagrams represent the same knot if and only if one can be deformed into the other via Reidemeister moves.*

By theorem 3, to show that a function on the set of link diagrams is a knot invariant, it suffices to prove that it is invariant under all three Reidemeister moves.

Definition 6. *An **oriented** link is simply a link whose components each have an associated orientation.*

We also have an oriented version of the Reidemeister theorem. A function on the set of oriented link diagrams that is invariant under all orientations of the three Reidemeister moves is an invariant of oriented links.

Many well-known knot and link invariants, like the crossing number and the unknotting number, or the volume of the complement, are difficult or even impossible to compute from a single diagram, but the following polynomial is very easy to compute given any oriented link diagram!

Definition 7. *Given any oriented link, the **bracket polynomial** is the polynomial resulting from repeated applications of the following two crossing resolution equations:*

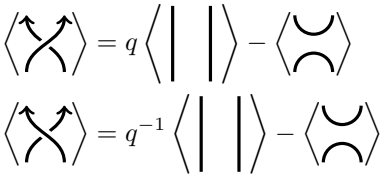

(1)

(2)

and the rules:

$$\langle D \sqcup \bigcirc \rangle = (q + q^{-1})\langle D \rangle \tag{3}$$

$$\langle \bigcirc \rangle = 1 \tag{4}$$

Note that applying these rules sometimes results in a link diagram whose orientation is only coherent near crossings. These are only formal orientations and we will only consider them temporarily while we do calculations.

Proposition 1. *The bracket polynomial is invariant under Reidemeister move II.*

Proof. For RII, we have

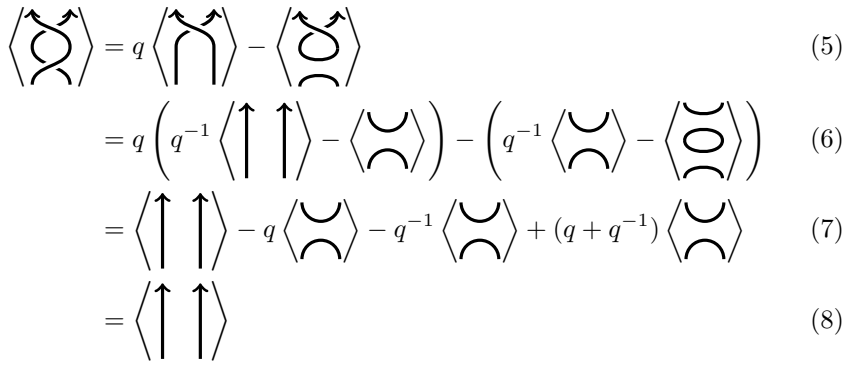

(5)–(8)

and in the other orientation,

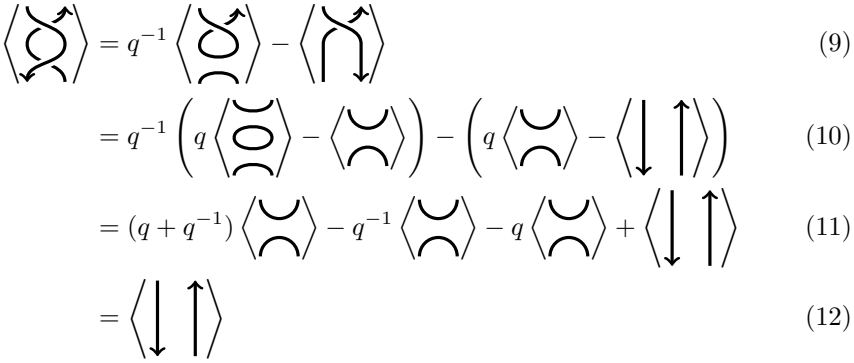

(9)–(12)

□

Proposition 2. *The bracket polynomial is invariant under Reidemeister move III.*

Proof. For RIII, we have a lot of options for orienting our strands. Luckily, we can get around having to check every possible orientation by making some observations about the bracket polynomial and cleverly applying RII, which we have proven for both possible orientations. First we will consider a version of RIII with a strand travelling behind a positive crossing. Note that

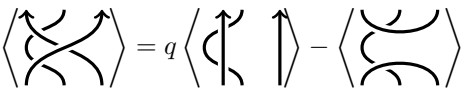

(13)

and

(14)

Now we can see that the right sides of equations (13) and (14) are equivalent, since

(15)

by two applications of proposition 1 (this works no matter how we orient the third strand), and

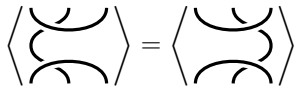

(16)

because the two diagrams are isotopic without interfering with any crossings. If instead we were moving a strand past a negative crossing, we would get

(17)

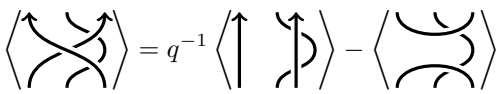

(18)

and the right hand sides would again be equivalent by the arguments above. □

The bracket polynomial is not quite a knot invariant. As we will see below, it is not invariant under RI.

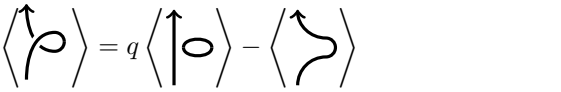

(19)

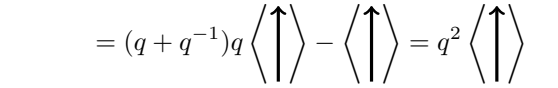

(20)

However, with a little adjustment, we can make the bracket polynomial a knot invariant. Since it is already invariant under Reidemeister moves II and III, we need only account for Reidemeister move I, which we will accomplish using the writhe.

Definition 8. *The* ***writhe*** *of a link diagram $w(D)$ is its number of positive crossings minus its number of negative crossings, where a positive crossing is given by*

and a negative crossing is given by

.

Note that in the counterexample above for RI, the crossing was positive. If we had instead used a loop with a negative crossing, we would have arrived at

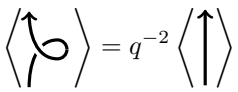

(21)

Thus we will guess that

Proposition 3. *$q^{-2w}\langle D\rangle$ is a link invariant where $\langle D\rangle$ is the bracket polynomial of a diagram D and w is its writhe.*

Proof. We already know that $\langle D\rangle$ is invariant under RII and RIII, and it is not too hard to see that the writhe is also preserved under all orientations of these moves. So we only have to show that $q^{-2w}\langle D\rangle$ is invariant under RI. Finally,

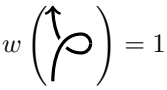

(22)

and

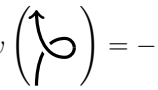

(23)

so

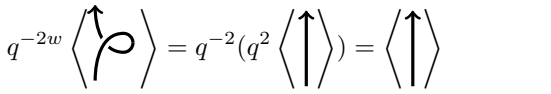

(24)

and

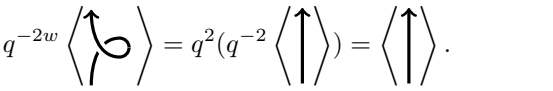

(25)

Thus, $q^{-2w}\langle D\rangle$ is invariant under all three Reidemeister moves and is thus a knot invariant. □

Definition 9. *The **Jones polynomial** $J(K)$ of a knot K is given by $q^{-2w}\langle D\rangle$ where D is any diagram of K and w is its writhe and where $\langle D\rangle$ is the bracket polynomial of D.*

Note that both the Jones polynomial and the bracket polynomial are Laurent polynomials, that is, they are polynomials in q and q^{-1}. This will become important later as we study the Jones polynomial more closely and plug in $e^{\frac{\pi i}{N}}$ for q. Since the Jones polynomial is a Laurent polynomial, as long as we plug in a non-zero value for q, we are not in any danger of dividing by zero.

Given any oriented link, the Jones polynomial is also given by recursive applications of the following Skein relation:

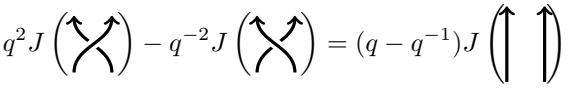

(26)

This follows immediately from the definition by algebraic manipulation of the two crossing resolution equations in the definition of the bracket polynomial. This formula and the rule $\langle D \rangle = 1$ can be used inductively to calculate the Jones polynomial of any knot because we know that every knot can be unknotted by changing crossings. As an example, we will now calculate the Jones polynomial of the figure eight knot using the skein relation.

$q^2 J$ 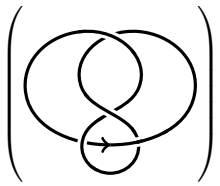 $- q^{-2} J$ 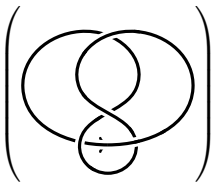 $= (q - q^{-1}) J$ 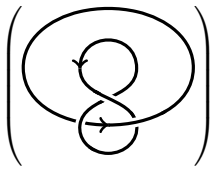

(27)

$-q^{-2} J$  $+ q^2 J$  $= (q - q^{-1}) J$ 

(28)

If we call the figure eight knot E and the Hopf link (the one at the left in the second equation and also the one on the right in the first equation) H, we have

$$q^2 J(E) - q^{-2} = (q - q^{-1}) J(H) \tag{29}$$

$$-q^{-2} J(H) + q^2 (q + q^{-1}) = q - q^{-1} \tag{30}$$

Solving for $J(H)$ and then plugging back into equation 30, we arrive at

$$J(H) = q + q^5 \tag{31}$$

$$J(E) = q^{-4} - q^{-2} + 1 - q^2 + q^4 \tag{32}$$

So far we have only defined the Jones polynomial using the bracket polynomial, but to generalize it into the colored Jones polynomial, it will be useful to also define the Jones polynomial algebraically using the braid group, which we will discuss in the next section.

2.1 The Braid Group

Definition 10. *An **n-braid** is an equivalence class (modulo ambient isotopy) of n smoothly embedded intervals (or strands) in $\mathbb{R}^2$ that start from n fixed points and go to another n fixed points such that their tangent vectors at all points are upwards, with crossings allowed.*

As with knots, we often represent braids by diagrams which project them generically down to a plane diagram with crossing information.

Definition 11. *The **braid group** B_n is the set of all n-braids together with the operation of stacking braids, that is, putting one braid directly on top of another so that the strands line up, creating a composite braid.*

A theorem due to Artin gives that the braid group is generated by $\{\sigma_1, \cdots, \sigma_n\}$ with relations $\sigma_i\sigma_j = \sigma_j\sigma_i$ $(|i-j|>1)$ and $\sigma_k\sigma_{k+1}\sigma_k = \sigma_{k+1}\sigma_k\sigma_{k+1}$ where σ_i is given by straight segments everywhere except the ith and $i+1$th strands, which make a positive crossing. σ_i^{-1} is σ_i with a negative crossing instead of a positive crossing.

By "closing" a braid, that is, connecting the n points at the top to the n points at the bottom, we arrive at a knot or link diagram. It is a theorem of Alexander that any knot or link can be represented by a braid. Markov proved the following theorem, which will help us to use braids to find knot and link invariants.

Theorem 4. *Two braids β and γ present the same knot or link if and only if they are related by a finite sequence of conjugations, stabilizations, and destabilizations, where a conjugation replaces $\alpha\beta$ with $\beta\alpha$, a stabilization changes $\beta \in B_n$ into $\beta\sigma_n^{\pm 1} \in B_{n+1}$, and a destabilization reverses a stabilization.*

Remark 1. *Examining what we know so far about braids, this theorem is roughly equivalent to Reidemeister's theorem about Reidemeister moves. The relations on the braid group are versions of Reidemeister moves II and III, conjugations of braids are a special kind of ambient isotopies of their closures, and stabilizations and destabilizations are RI moves.*

2.2 Yang-Baxter Operators

Definition 12. *Let V be an N-dimensional vector space over $\mathbb{C}$, and R_N an automorphism of $V \otimes V$. Then R is a Yang-Baxter operator if*

$$(R_N \otimes I_N)(I_N \otimes R_N)(R_N \otimes I_N) = (I_N \otimes R_N)(R_N \otimes I_N)(I_N \otimes R_N) \tag{33}$$

where I_N is the identity operator in V. We frequently refer to R simply as the R matrix.

Yang-Baxter operators can be used to define link invariants. Given an n-braid β, replacing σ_i with $I_V^{\otimes(i-1)} \otimes R \otimes I_V^{\otimes(n-i-1)}$ and σ_i^{-1} with $I_V^{\otimes(i-1)} \otimes R^{-1} \otimes I_V^{\otimes(n-i-1)}$ results in a homomorphism $\phi(\beta)$ from $V^{\otimes n}$ to itself. By equation 33, the homomorphism $\phi(\beta)$ is an invariant of braids because it is invariant under the relation $\sigma_k\sigma_{k+1}\sigma_k = \sigma_{k+1}\sigma_k\sigma_{k+1}$.

Theorem 5. *Let R be a Yang-Baxter operator, β an n-braid, and $\phi(\beta)$ as described above. Then if μ is an automorphism of V and q is a non-zero complex number such that*

$$R(\mu \otimes \mu) = (\mu \otimes \mu)R \tag{34}$$

$$\mathrm{Tr}_2(R^{\pm 1}(I_N \otimes \mu)) = q^{\pm 2} I_N, \tag{35}$$

we have that

$$T_{R,\mu}(\beta) = q^{-2w(\beta)} \,\mathrm{Tr}_1(\mathrm{Tr}_2(\cdots(\mathrm{Tr}_n(\phi(\beta)\mu^{\otimes n}))\cdots)) \tag{36}$$

is a link invariant, where

$$\mathrm{Tr}_k(f)(e_{i_1}\otimes e_{i_2}\cdots\otimes e_{i_{k-1}}) = \sum_{j_1,j_2,\cdots,j_{k-1},j=0}^{N-1} f_{i_1,i_2,\cdots,i_{k-1},j}^{j_1,j_2,\cdots,j_{k_1},j}(e_{j_1}\otimes e_{j_2}\otimes\cdots\otimes e_{j_{k-1}}\otimes e_j) \tag{37}$$

for f given by

$$f(e_{i_1}\otimes e_{i_2}\otimes\cdots\otimes e_{i_k}) = \sum_{j_1,j_2,\cdots,j_k=0}^{N-1} f_{i_1,i_2,\cdots,i_k}^{j_1,j_2,\cdots,j_k}(e_{j_1}\otimes e_{j_2}\otimes\cdots\otimes e_{j_k}) \tag{38}$$

and $\{e_0,\cdots e_{N-1}\}$ a basis of V.

Proof. (sketch) By Markov's theorem (theorem 4), it suffices to show that $T_{R,\mu}$ is invariant under a conjugation and a stabilization. The invariance under a conjugation follows from $(\mu\otimes\mu)R = R(\mu\otimes\mu)$ (i.e., the condition that $\mu\otimes\mu$ can pass through a crossing). Finally, the invariance under stabilizations follows from $\mathrm{Tr}_2(R^{\pm1}(I_N\otimes\mu)) = q^{\pm2}I_N$. □

Proposition 4. *Let $V=\mathbb{C}^2$ and let*

$$R = \begin{bmatrix} q & 0 & 0 & 0 \\ 0 & q-q^{-1} & 1 & 0 \\ 0 & 1 & 0 & 0 \\ 0 & 0 & 0 & q \end{bmatrix} \tag{39}$$

$$\mu = \begin{bmatrix} q^{-1} & 0 \\ 0 & q \end{bmatrix} \tag{40}$$

Then $T_{R,\mu}$ gives a version of the Jones polynomial.

Proof. We can see that R satisfies

$$R - R^{-1} = (q-q^{-1})(I\otimes I). \tag{41}$$

We can represent the knots from the Jones skein by the braids $\beta\sigma_i\beta'$, $\beta\sigma_i^{-1}\beta'$ and $\beta\beta'$, so to check the Jones skein we will take

$$\begin{aligned}
&q^2T_{R,\mu}(\beta\sigma_i\beta') - q^{-2}T_{R,\mu}(\beta\sigma_i^{-1}\beta') \\
&= q^2q^{-2(w(\beta\beta')+1)}\,\mathrm{Tr}_1(\cdots(\mathrm{Tr}_n(\phi(\beta\sigma_i\beta')\mu^{\otimes n}))\cdots) && (42)\\
&- q^{-2}q^{-2(w(\beta\beta')-1)}\,\mathrm{Tr}_1(\cdots(\mathrm{Tr}_n(\phi(\beta\sigma_i^{-1}\beta')\mu^{\otimes n}))\cdots) \\
&= q^{-2w(\beta\beta')}\,\mathrm{Tr}_1(\cdots(\mathrm{Tr}_n(\phi(\beta I_2^{\otimes(i-1)}\otimes R\otimes I_2^{\otimes(n-i-1)}\beta')\mu^{\otimes n}))\cdots) \\
&- q^{-2w(\beta\beta')}\,\mathrm{Tr}_1(\cdots(\mathrm{Tr}_n(\phi(\beta I_2^{\otimes(i-1)}\otimes R^{-1}\otimes I_2^{\otimes(n-i-1)}\beta')\mu^{\otimes n}))\cdots) && (43)\\
&= q^{-2w(\beta\beta')}\,\mathrm{Tr}_1(\cdots(\mathrm{Tr}_n(\phi(\beta I_2^{\otimes(i-1)}\otimes(q-q^{-1})(I_2\otimes I_2)\otimes I_2^{\otimes(n-i-1)}\beta')\mu^{\otimes n}))\cdots) && (44)\\
&= (q-q^-1)T_{R,\mu}(\beta\beta') && (45)
\end{aligned}$$

so $T_{R,\mu}$ does indeed satisfy the Jones skein for $V = \mathbb{C}^2$ and the above values of R and μ. However, since the closure of the braid

(46)

is the unknot, we can see that $T_{R,\mu}(\bigcirc)$ is $\mathrm{Tr}_1(I\mu) = q + q^{-1}$, so we have that with the above hypotheses, $T_{R,\mu}$ gives a version of the Jones polynomial with $J(\bigcirc) = q + q^{-1}$ instead of $J(\bigcirc) = 1$. □

Using deformations of Lie algebras called quantum groups (this deformation is where the complex number q arises), one can define other Yang-Baxter operators and by theorem 5 generate other link invariants. The most important of these for us is the colored Jones polynomial $J(N; q)$, which is defined using the Lie algebra $\mathrm{sl}_2(\mathbb{C})$ and its N-dimensional irreducible representation. If $N = 2$, we recover the ordinary Jones polynomial.

3 Decomposition of Knot Complements

To calculate the volume of the complement of a knot we will need to be able to first break that knot complement into ideal tetrahedra whose hyperbolic volume we understand well. For that, we will start by breaking the knot complement into two ideal polyhedra and then we will further break up our two polyhedra into ideal tetrahedra. In other words, our end goal is to have a delta compex of the knot complement whose vertices are not in the space (because they are on the knot). Recall that a knot is an embedding of $\mathbb{S}^1$ into $\mathbb{S}^3$. We think of $\mathbb{S}^3$ as $\mathbb{R}^3$ plus a point at infinity.

Start with a knot diagram. We will think of it as a 3-dimensional knot residing in a neighborhood of a plane which we are looking down on from above. Imagine blowing up two balloons, one above the knot diagram and one below it. They will meet in the areas between strands of the knot diagram and form faces, which will meet at edges. We will have one edge for each crossing, which we will realize as an arrow going vertically down from the top strand to the bottom strand at every crossing. In the space we want to decompose, the knot does not exist, so the knot itself does not contribute any edges to the decomposition! Four faces meet at every crossing and share an edge as depicted in figure 2, where the bold lines are strands of the knot diagram.

Once we have a knot diagram with edges inserted, we will shrink the knot to ideal vertices. Remember that the knot is not part of the space we want to decompose, and so the strands of the knot diagram are not edges in our decomposition but instead vertices that we view as ideal vertices, i.e. vertices at infinity. To draw this, it is helpful to draw four copies of each edge, one in each corner of a crossing, as in figure 3. For the top polyhedron, we are imagining that we are inside of the balloon that expands outward until it reaches the knot, looking downwards at the knot diagram. Accordingly, the edges that are isotopic by sliding their tail along the over strand at each crossing will merge in our diagram of the top polyhedron. This is shown for the figure eight knot

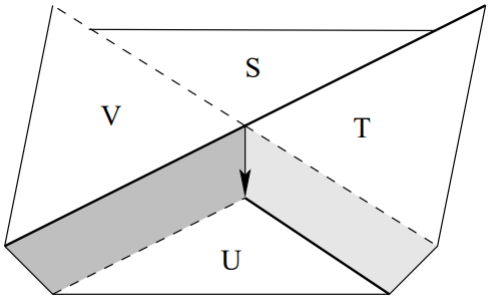

Figure 2: A crossing in the polyhedral decomposition of a knot. The arrow is an edge in the decomposition where the faces S, T, U, and V meet. Figure taken from [1]

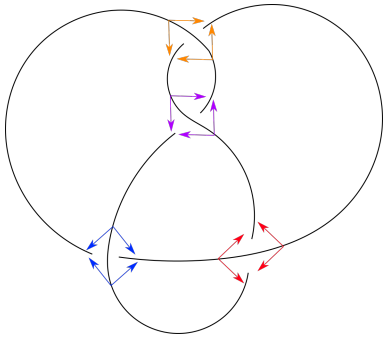

Figure 3: A figure eight knot diagram with four copies of each edge in the decomposition drawn in at the crossings.

in figure 4. When the strands of the knot diagram shrink to points, we are left with the diagram in figure 5. For the bottom polyhedron, the balloon is expanding upwards towards the knot, and so in its perspective, what look like under strands to us are its over strands. So for the bottom polyhedron diagram we will merge edges that are isotopic by sliding their heads along the under strands, then shrink the "over" strands just as before (except they will be under strands in the knot diagram from our perspective). This is shown for the figure eight knot in figure 6.

The next step is to eliminate bigons from the decomposition. These are "polygons" with only two edges and two vertices. To eliminate the bigons in the polyhedra we have drawn for the figure eight knot, we switch the orientation of the orange edge and merge it with the purple edge and switch the orientation of the blue edge and merge it with the red edge. We can visualize this process as squishing a football-shaped disk down into a segment The result is shown in figures 7 and 8.

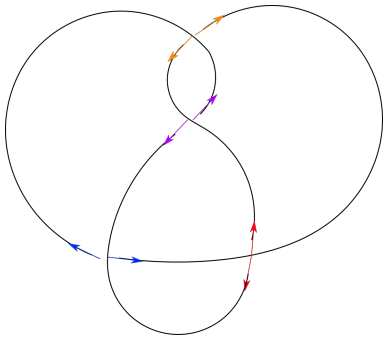

Figure 4: The figure eight knot diagram with edges that are isotopic along the over strands merged.

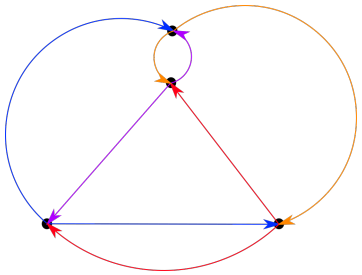

Figure 5: A diagram of the top polyhedron in the decomposition of the figure eight knot complement

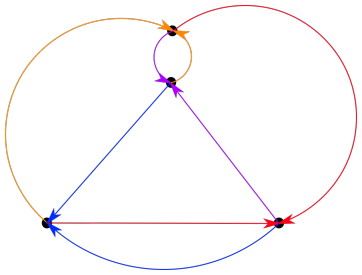

Figure 6: A diagram of the bottom polyhedron in the decomposition of the figure eight knot complement

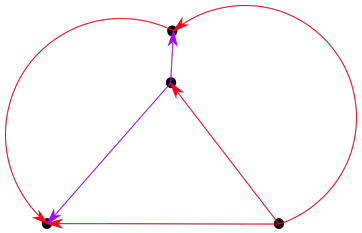

Figure 7: The top polyhedron with bigons removed.

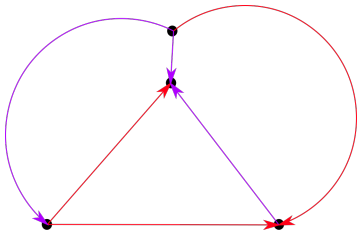

Figure 8: The bottom polyhedron with bigons removed.

For the figure eight knot, we are done because we have a decomposition that gives two ideal tetrahedra, from which we can easily compute lots of information about the structure of the knot complement. However, for more elaborate knots and links, we would likely still have two fairly complicated ideal polyhedra, not all of whose sides would be triangles. In that event, we would subdivide non-triangle sides into triangles, then break the two polyhedra into tetrahedra. However, it is not known whether every hyperbolic knot complement has a delta complex decomposition in which each tetrahedron has a hyperbolic structure and the result of the gluing is a smooth hyperbolic 3-manifold with a complete metric, so this strategy may not work for finding the hyperbolic structure of every knot (we may need to stick to larger ideal polyhedra in some cases. See [1]).

4 Hyperbolic Structure

4.1 Hyperbolic Geometry

Although we are most concerned with three-dimensional hyperbolic geometry, it will be illustrative to first state a few facts about the hyperbolic plane, $\mathbb{H}^2$. We study this geometry using the half-plane model, in which the hyperbolic plane $\mathbb{H}^2$ consists of the points in the upper half plane $\{x + iy \in \mathbb{C} | y > 0\}$ equipped with the metric

$$ds^2 = \frac{dx^2 + dy^2}{y^2}.$$

The geodesics (distance-minimizing curves) in this geometry are semi-circles

whose centers lie on the real axis (the boundary of $\mathbb{H}^2$ in this model) and straight lines that are perpendicular to it.

Its isometries are all given by compositions of inversions through these geodesics, just as the isometries of the Euclidean plane are given by compositions of reflections through lines.

Definition 13. *An **ideal point** is any point on the real line plus the point at infinity, that is, a point on the boundary of $\mathbb{H}^2$.*

Definition 14. *An **ideal triangle** is a triangle in $\mathbb{H}^2$ all of whose vertices are ideal.*

Definition 15. *A **horocycle** is a circle in the upper half plane which is tangent to the real line. Equivalently, a horocycle is a curve which is perpendicular to every geodesic through a certain ideal point, its center.*

Just as with $\mathbb{H}^2$, we study $\mathbb{H}^3$ via a half-space model. Our model of $\mathbb{H}^3$ consists of the points in $\{(x+iy, w) \in \mathbb{C} \times \mathbb{R} | w > 0\}$ equipped with the metric

$$ds^2 = \frac{dx^2 + dy^2 + dw^2}{w^2}.$$

As with $\mathbb{H}^2$, we sometimes need to consider the points on the boundary of $\mathbb{H}^3$.

Definition 16. *An **ideal point** of $\mathbb{H}^3$ is any point in $\mathbb{C} \cup \infty$, the boundary of $\mathbb{H}^3$.*

Just as there are copies of $\mathbb{R}^2$ within $\mathbb{R}^3$, copies of $\mathbb{H}^2$ exist in $\mathbb{H}^3$. They are are analogous to planes in $\mathbb{R}^3$ in that a curve minimizing the distance between two points on one of them also minimizes the distance between those points in the higher-dimensional space. These copies of $\mathbb{H}^2$ in $\mathbb{H}^3$ are called **totally geodesic surfaces** and they are given by planes and hemispheres perpendicular to the boundary in our model.

Just as we might expect from the two-dimensional case, isometries of $\mathbb{H}^3$ are given by compositions of reflections through these totally geodesic surfaces. In practice, we will only want to consider the orientation-preserving isometries of $\mathbb{H}^3$, and we are most interested in how they act on the boundary. The elements of the group of Möbius transformations $\mathrm{PSL}(2, \mathbb{C})$, that is, transformations of the form

$$z \mapsto \frac{az + b}{cz + d} \tag{47}$$

where $a, b, c, d \in \mathbb{C}$ and $ad - bc \neq 0$ are the group of orientation-preserving isometries of $\mathbb{C} \cup \infty$. Each of them is a composition of an even number of inversions through lines and circles in $\mathbb{C} \cup \infty$ (the fact that the number of inversions is even guarantees that the orientation is preserved). Since every line and circle in $\mathbb{C} \cup \infty$ uniquely determines a plane or hemisphere perpendicular to the

boundary, the elements of $\mathrm{PSL}(2,\mathbb{C})$ can naturally be extended to act on all of $\mathbb{H}^3$. One simply decomposes each element down into its inversions through lines and circles in the boundary, then instead performs those inversions through the corresponding planes and hemispheres perpendicular to the boundary. Hence we will think of Möbius transformations as orientation-preserving isometries of $\mathbb{H}^3$ and use them to calculate the effect of isometries on ideal points.

Given any three (ideal) points z_1, z_2, and z_3, the Möbius transformation

$$f(z) = \frac{(z - z_1)(z_2 - z_3)}{(z - z_3)(z_2 - z_1)} \tag{48}$$

takes z_1 to 0, z_2 to 1, and z_3 to ∞. Given an arbitrary Möbius transformation

$$f(z) = \frac{az + b}{cz + d}, \tag{49}$$

$$f^{-1}(z) = \frac{dz - b}{-cz + a} \tag{50}$$

gives the inverse transformation. It follows that a Möbius transformation is determined by where it sends three points, hence an isometry of $\mathbb{H}^3$ is determined by where it sends three ideal points.

Definition 17. *An **ideal tetrahedron** is a tetrahedron whose vertices are all ideal points.*

Definition 18. *A **horosphere** about an ideal point $p \in \mathbb{C} \cup \infty$ is a surface that is perpendicular to all geodesics through p. Equivalently, a horosphere is a Euclidean sphere tangent to p (or a plane parallel to $\mathbb{C}$ if $p = \infty$).*

The induced metric on a horosphere is Euclidean, and the intersection of a horosphere centered at a vertex of an ideal tetrahedron with the tetrahedron is a Euclidean triangle. This is easiest to picture when the ideal vertex is at ∞, as in figure 9.

4.2 Gluing Equations

Definition 19. *Let M be a three-manifold. We say that M has a hyperbolic structure if for ever point $x \in M$ there exists a neighborhood of x which is isometric to an open ball in $\mathbb{H}^3$.*

If we have such an isometry for every point in M, we can induce a hyperbolic metric on M.

Definition 20. *We say that a manifold M with a hyperbolic structure has a **complete** hyperbolic structure if the metric induced on M is complete.*

Given a triangulation of a knot complement, is it possible to put a complete hyperbolic structure on it? One way to endow our manifold with such a structure

is to view each tetrahedron as an ideal tetrahedron in $\mathbb{H}^3$ and glue the ideal tetrahedra together in a compatible way. First, we will need to make sure that we glue the ideal tetrahedra in our triangulation together in a way that is locally isometric to $\mathbb{H}^3$ at every point. Inside of the ideal tetrahedra we know that this is true for every point, but we need to make sure that everything glues up nicely around each edge so that neighborhoods of points on faces and edges of the ideal tetrahedra are also isometric to balls in $\mathbb{H}^3$. Let us examine what happens around one edge, e, in a gluing of ideal tetrahedra.

First, suppose that we have identified the interior of each tetrahedron in our decomposition with an ideal tetrahedron in $\mathbb{H}^3$. Place e in $\mathbb{H}^3$ so that one ideal vertex is at 0 and the other is at ∞. Now take an ideal tetrahedron T_1 with an edge that glues to e (call it e_1) and place it in $\mathbb{H}^3$ so that one of its two remaining ideal vertices is at 1 and the last ideal vertex is at some point z_1 in the complex plane where $\mathrm{Im}(z) > 0$. We can always place an ideal tetrahedron in this position and the number z_1 will always be the same because an isometry of $\mathbb{H}^3$ is determined by where it sends three points.

Definition 21. *In the process described above, z_1 or $z(e_1)$ is called the **edge invariant** of e_1 in T_1.*

Now, take the tetrahedron T_2 that glues to T_1 along the face between e and z_1 and place it in $\mathbb{H}^3$ so that the edge e_2 that glues to e goes between 0 and ∞, another ideal vertex goes to z_1, and the two tetrahedra do not overlap. The edge e_2 in T_2 has an edge invariant, $e(z_2)$. The Möbius transformation taking 1 to $e(z_1)$ and fixing 0 and ∞ is given by $f(w) = z(e_1)w$, so the fourth ideal vertex of T_2 must now be at $z(e_1)z(e_2)$. By a similar argument, if T_3 glues to T_2 along the face between 0, ∞, and $z(e_1)z(e_2)$, its fourth vertex must be at $z(e_1)z(e_2)z(e_3)$ and the fourth vertex of T_n must be at $z(e_1)z(e_2)\cdots z(e_n)$. Now, if T_n glues back to T_1, for the gluing to give a hyperbolic structure, it must be that its fourth vertex is at 1. If T_n does not have its fourth vertex at 1, then the last face of T_n does not glue to a face in our triangulation and our gluing is not valid. Thus, for our gluing to give a hyperbolic structure we must have

$$\prod_{i=1}^{n} z(e_i) = 1 \tag{51}$$

We also want to make sure that the sum of the angles around a point on an edge in a hyperspherical cross section of the gluing is 2π, that is to say, that our tetrahedra wrap around each edge exactly one time. This gives the other gluing equation,

$$\sum_{i=1}^{n} \arg(z(e_i)) = 2\pi$$

At first glance it would seem that we have six unknowns for each tetrahedron

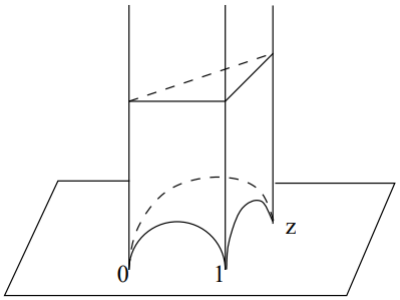

Figure 9: An ideal tetrahedron in standard position. Figure taken from [1]

in each of these sets of equations, one for each edge of the tetrahedron. But, as we will see, one edge invariant determines the other five.

Take a tetrahedron and place it in the standard position, that is, put one ideal vertex at 0, one at 1, and one at ∞, and if the fourth vertex has negative imaginary part, use an isometry to fix 0 and ∞ and send the fourth vertex to 1 so that 1 is sent to a point z such that $\mathrm{Im}(z) > 0$, as in figure 9. Now z is the edge invariant of the edge from 0 to ∞, which we will call e_1. Label the edge from 1 to ∞ e_2 and the edge from z to ∞ e_3. To find the edge invariant of e_2 we must put e_2 in the position of e_1 via isometry while keeping our ideal tetrahedron in standard position. Thus we need the Möbius transformation defined by

$$w \mapsto \frac{w-1}{z-1},$$

which fixes ∞, sends 1 to 0, and sends z to 1. The transformation sends 0 to $\frac{1}{1-z}$, which becomes our new "fourth" vertex (i.e., the one that is not 0, 1, or ∞) so the edge invariant of e_2 is $\frac{1}{1-z}$. Next we want to apply an isometry of $\mathbb{H}^3$ to our original tetrahedron to find the edge invariant of e_3. This isometry is given by

$$w \mapsto \frac{w-z}{-z},$$

which fixes ∞, sends z to 0, and sends 0 to 1, thus sending e_3 to e_1 and keeping the tetrahedron in standard position. This isometry takes 1 to $\frac{1-z}{-z}$, which is our new "fourth" vertex, so the edge invariant of e_3 is $\frac{z-1}{z}$. There are still three edges whose invariants we have not yet found, but they are the same three invariants as the ones we just found, as will now show in a lemma.

Lemma 1. *Opposite edges in an ideal tetrahedron have the same edge invariant.*

Proof. Take a tetrahedron in standard position whose edge at 0 has edge invariant z. It suffices to show that the edge invariant of the edge e' between 1

and z, the opposite edge to the one at 0, also has edge invariant z. We need an isometry that takes that edge to the edge between 0 and ∞. It is given by

$$w \mapsto \frac{zw - z}{w - z},$$

since this is the isometry that takes z to ∞, 1 to 0, and 0 to 1. This isometry takes ∞ to z, so the edge invariant of e' is z, as was to be shown. □

Together, the two sets of gluing equations guarantee that our gluing induces a hyperbolic structure on our topological ideal triangulation. But recall that for our gluing to give a geometric triangulation (i.e., one which we could use to calculate the hyperbolic volume of the knot complement), we need the hyperbolic structure to be complete. Thus we need a condition that guarantees that the hyperbolic structure on an ideal triangulation of a knot complement is complete.

4.3 Completeness Equations

To check whether a given manifold satisfying the gluing equations has a complete hyperbolic structure we will examine its cusps.

Definition 22. *A **cusp** of a 3-manifold is the surface of a horosphere centered at an ideal vertex of the manifold intersected with the manifold.*

Suppose that we have a decomposition of a knot complement into ideal tetrahedra that satisfies the gluing equations and that we have glued into $\mathbb{H}^3$ in such a way that it has a vertex at ∞. Then a cusp of ∞ in the glued manifold will be a plane parallel to the boundary plane intersected with the manifold. The gluing tells us to enter back into the other side of the gluing every time we get to a face of a tetrahedron as we move through the gluing. The gluing lives in $\mathbb{H}^3$, so it must be orientable. So topologically, the intersection between the horocycle and the knot decomposition is a torus. We might also think of the horosphere as thickening up the knot which we have pushed out to infinity and which is in some sense the vertex of our manifold. The knot is a copy of $\mathbb{S}^1$, so we should expect this formal "thickening" of it to result in a torus.

Theorem 6. *Let M be a three-manifold with hyperbolic structure and ideal torus boundary. Then if the induced structure on a cusp of every ideal vertex is Euclidean, the hyperbolic structure on M is complete (see [1]).*

This theorem may seem mysterious at first, but keep in mind that, after gluing, knot complements are three-manifolds with ideal torus boundary (the point at infinity that the knot shrinks to!).

Definition 23. *We call the intersection of a cusp with a delta complex of the manifold a **cusp triangulation**.*

Since we know that the intersection of a horosphere centered at a vertex of an ideal tetrahedron with the ideal tetrahedron is a Euclidean triangle whose angles are the dihedral angles of the tetrahedron (the arguments of its edge invariants), we can see immediately that, given an ideal triangulation of a manifold and an ideal vertex, the cusp triangulation is unique up to scaling, i.e., every cusp triangulation is similar to every other. So if the structure on one cusp of an ideal vertex turns out to be complete, it will be complete for every cusp.

Consider a triangulation of a cusp T. Let e be a directed edge in T. Now take a smooth loop $\alpha \in \pi_1(T)$ that goes through e. We will associate a complex number $H(\alpha)$ to α by the following algorithm.

Set $H = 1$. Follow α to another copy of e in the triangulation. Find a way to move the first copy of e to the second by a sequence of rotations about vertices in the cusp triangulation, to which will naturally be associated edge invariants from the ideal triangulation. If you rotate clockwise about a vertex whose edge invariant is z, replace H by $\frac{H}{z}$. If you rotate counterclockwise instead, replace H by zH. If at the end, the orientation of e has flipped, multiply H by -1. $H(\alpha)$ is defined as the final value of H in this process.

Proposition 5. *If α and β generate $\pi_1(T)$ and $H(\alpha) = H(\beta) = 1$ then the hyperbolic structure on the knot complement is complete.*

Proof. (sketch) By theorem 6, it suffices to show that the structure on T is Euclidean. If $H(\alpha) = H(\beta) = 1$ then edges of triangles in the triangulation of T are not rotated, scaled, or reflected when they are taken by holonomy to their copies. Thus the triangles themselves are not rotated, scaled, or reflected when they are taken by holonomy to their copies. Thus the holonomy group is generated by Euclidean translations and so the structure on T is indeed Euclidean and complete. (For a more detailed proof and an explanation of holonomy, see [1]) □

Now that we have laid out the process of finding gluing and completeness equations for a decomposition of a knot complement, let us try to find and solve them for the figure eight knot to demonstrate the process in action.

By examining figure 10, we arrive at the following gluing equation for the red edge:

$$z_1^2 z_2 v_3^2 v_2 = 1 \tag{52}$$

For the purple edge, we have

$$z_3^2 z_2 v_1^2 v_2 = 1 \tag{53}$$

After setting $z_1 = z$, $z_2 = \frac{1}{1-z}$, $z_3 = \frac{z-1}{z}$, and the v_i's similarly, we get,

$$\frac{z^2(v-1)^2}{(1-z)v^2(1-v)} = 1 \tag{54}$$

$$\frac{(z-1)^2 v^2}{z^2(1-z)(1-v)} = 1 \tag{55}$$

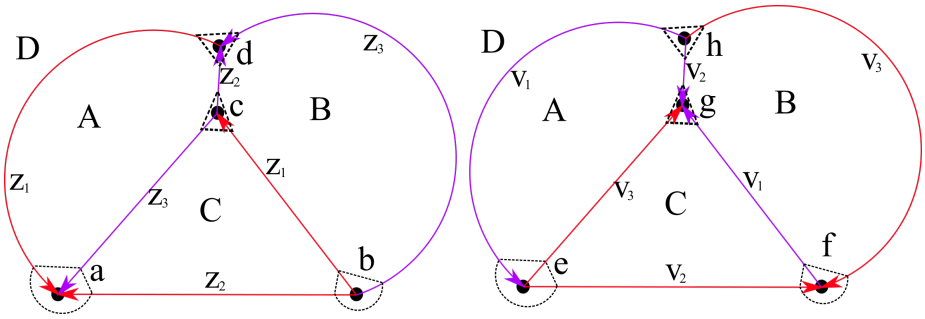

Figure 10: The two tetrahedra in the figure eight knot complement with triangles formed by the intersection of a horosphere drawn in around the ideal vertices

From figure 10 we can read off a cusp triangulation. Part of this triangulation is given in figure 11, where we can read off the following two completeness equations:

$$z_2 v_2^{-1} z_3 v_1^{-1} z_2 v_2^{-1} z_3 v_1^{-1} = 1 \tag{56}$$

$$v_2^{-1} z_2 v_3^{-1} z_1 v_2^{-1} z_2 v_3^{-1} z_1 = 1 \tag{57}$$

or, writing everything in terms of v and z,

$$\frac{(1-v)^2(z-1)^2}{(1-z)^2 z^2 v^2} = 1 \tag{58}$$

$$\frac{(1-v)^2 v^2 z^2}{(1-z)^2 (v-1)^2} = 1. \tag{59}$$

These last two give us

$$(1-v)^2 = z^2 v^2 \tag{60}$$

$$v^2 z^2 = (1-z)^2. \tag{61}$$

Combining these, we get

$$(1-v)^2 = (1-z)^2. \tag{62}$$

This is solved by either $z = v$ or $z = 2 - v$. However, we must throw out $z = 2 - v$ because we need z and v to both have positive imaginary parts. Therefore we will take $z = v$ and reexamine the completeness equations. Equation 56 becomes

$$(1-z)^2 = z^4, \tag{63}$$

which has solutions $z = -\frac{1}{2} - \frac{\sqrt{5}}{2}$, $z = \frac{\sqrt{5}}{2} - \frac{1}{2}$, $z = \sqrt[3]{-1}$, and $z = -(\sqrt[3]{-1}^2)$. Of these, only $z = \sqrt[3]{-1}$ has positive imaginary part, so the completeness equations tell us that the only complete hyperbolic structure on our ideal triangulation is the one given by $v = z = \sqrt[3]{-1}$. We can see that

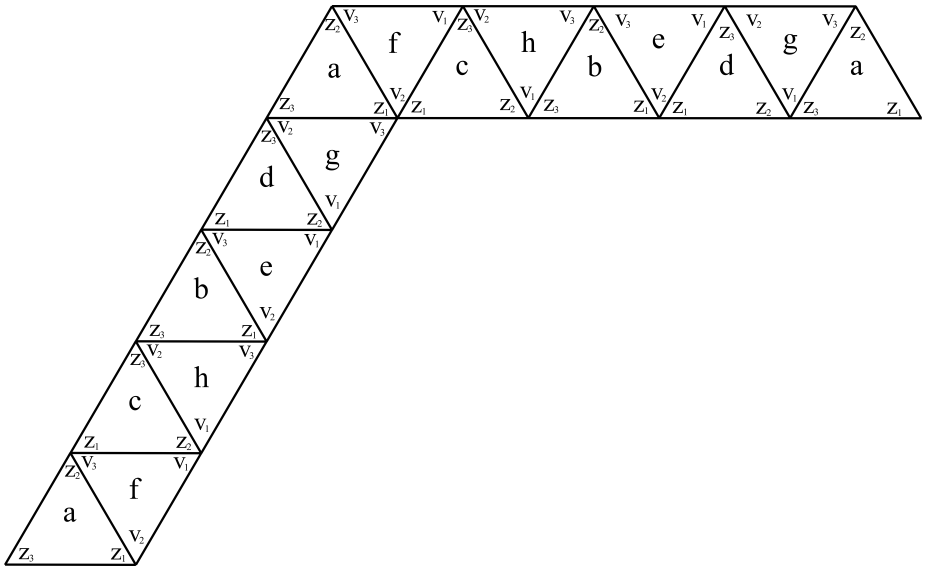

Figure 11: Part of a cusp of the figure eight knot complement with its triangulation drawn in

$$\sqrt[3]{-1} = e^{\frac{i\pi}{3}} = \frac{1}{2} + \frac{i\sqrt{3}}{2} \tag{64}$$

and

$$z_2 = \frac{1}{1 - (\frac{1}{2} + \frac{i\sqrt{3}}{2})} = \frac{1}{\frac{1}{2} - \frac{i\sqrt{3}}{2}} = \frac{\frac{1}{2} + \frac{i\sqrt{3}}{2}}{1} \tag{65}$$

$$z_3 = \frac{\frac{1}{2} + \frac{i\sqrt{3}}{2} - 1}{\frac{1}{2} + \frac{i\sqrt{3}}{2}} = \frac{-\frac{1}{2} + \frac{i\sqrt{3}}{2}}{\frac{1}{2} + \frac{i\sqrt{3}}{2}} \frac{\frac{1}{2} - \frac{i\sqrt{3}}{2}}{\frac{1}{2} - \frac{i\sqrt{3}}{2}} = \frac{\frac{1}{2} + \frac{i\sqrt{3}}{2}}{1} \tag{66}$$

So in fact every edge invariant in the decomposition is $\frac{1}{2} + \frac{i\sqrt{3}}{2}$, and since $\arg(\frac{1}{2} + \frac{i\sqrt{3}}{2}) = \frac{\pi}{3}$, we can see that the two ideal tetrahedra in our decomposition are both regular. As we will see in the next subsection, now that we know the measures of the dihedral angles in the tetrahedra (the angles between the faces), we can calculate their volumes!

4.4 The Lobachevsky Function and Volumes of Ideal Tetrahedra

Definition 24. *The* ***Lobachevsky function*** $\Lambda(\theta)$ *is defined by*

$$\Lambda(\theta) = -\int_0^\theta \log|2\sin(x)|dx \tag{67}$$

for $\theta \in \mathbb{R}$.

Some properties of the Lobachevsky function are given in the following three propositions.

Proposition 6. *For* $0 \leq \theta \leq \pi$, *the Lobachevsky function has uniformly convergent Fourier series expansion*

$$\Lambda(\theta) = \frac{1}{2} \sum_{n=1}^{\infty} \frac{\sin(2n\theta)}{n^2} \tag{68}$$

Proof. Let $\psi(z)$ be the dilogarithm function defined by

$$\psi(z) = \sum_{n=1}^{\infty} \frac{z^n}{n^2} \tag{69}$$

for $|z| \leq 1$. Then we have

$$\psi'(z) = \sum_{n=1}^{\infty} \frac{z^{n-1}}{n} \tag{70}$$

$\log(1+z)$ has power series

$$\log(1+z) = \sum_{n=1}^{\infty} \frac{(-1)^{n-1} z^n}{n}, \tag{71}$$

so

$$\psi'(z) = -\frac{\log(1-z)}{z} \tag{72}$$

Since $\psi(0) = 0$, we have

$$\psi(z) = -\int_0^z \frac{\log(1-w)}{w} dw \tag{73}$$

so we have

$$\psi(e^{2i\theta}) - \psi(1) = -\int_1^{e^{2i\theta}} \frac{\log(1-w)}{w} dw \tag{74}$$

and by the substitution $w = e^{2i\theta}$, $dw = 2ie^{2i\theta}$ we arrive at

$$= -\int_0^{\theta} 2i \log(1 - e^{2i\theta}) d\theta = -\int_0^{\theta} 2i (\log(\frac{e^{i\theta} - e^{-i\theta}}{i}) + i\theta - \frac{i\pi}{2}) d\theta \tag{75}$$

$$= -\int_0^{\theta} 2i \log(2\sin(\theta)) - 2\theta + \pi d\theta = 2i\Lambda(\theta) + \left[\theta^2 - \pi\theta\right]_0^{\theta} \tag{76}$$

giving us the identity

$$\psi(e^{2i\theta}) - \psi(1) = 2i\Lambda(\theta) + \theta^2 - \pi\theta, \tag{77}$$

for $0 \leq \theta \leq \pi$. Taking the imaginary part of both sides, we have

$$\sum_{n=1}^{\infty} \frac{\sin(2n\theta)}{n^2} = 2\Lambda(\theta), \tag{78}$$

as was to be shown. □

Proposition 7. *The Lobachevsky function is odd and periodic with period π.*

Proof.

$$\Lambda(-\theta) = -\int_0^{-\theta} \log|2\sin(x)|dx = \int_{-\theta}^{0} \log|2\sin(x)|dx \tag{79}$$

We will make the change of variables $u = -x$, $du = -dx$ to obtain

$$-\int_{\theta}^{0} \log|2\sin(-u)|du = \int_0^{\theta} \log|2\sin(u)|du = -\Lambda(\theta) \tag{80}$$

since $\sin(x)$ is an odd function, so the Lobachevsky function is indeed odd. As for periodicity,

$$\Lambda(\theta+\pi) = -\int_0^{\theta+\pi} \log|2\sin(x)|dx \tag{81}$$

$$\Lambda'(\theta+\pi) = -\log|2\sin(\theta+\pi)| = -\log|-2\sin(\theta)| = -\log|2\sin(\theta)| \tag{82}$$

$$= \Lambda'(\theta) \tag{83}$$

so we have that $\Lambda(\theta)$ and $\Lambda(\theta+\pi)$ differ by a constant for all θ. Now we observe that using the Fourier expansion from proposition 6, $\Lambda(0) = 0$ and $\Lambda(\pi) = 0$, so the constant difference between $\Lambda(\theta)$ and $\Lambda(\theta+\pi)$ is 0, and we are done. □

Proposition 8. *For all θ we have*

$$\Lambda(2\theta) = 2\Lambda(\theta) + 2\Lambda\left(\theta + \frac{\pi}{2}\right) \tag{84}$$

Proof.

$$\Lambda(2\theta) = -\int_0^{2\theta} \log|2\sin(x)|dx = -2\int_0^{\theta} \log|2\sin(2u)|du \tag{85}$$

by the substitution $u = \frac{x}{2}$, $du = \frac{dx}{2}$.

$$= -2\int_0^{\theta} \log|4\sin(u)\cos(u)|du = -2\int_0^{\theta} \log|2\sin(u)|du - 2\int_0^{\theta} \log|2\cos(u)|du \tag{86}$$

$$= -2\int_0^{\theta} \log|2\sin(u)|du - 2\int_0^{\theta} \log\left|2\sin\left(u + \frac{\pi}{2}\right)\right|du \tag{87}$$

In the integral on the right we will make the substitution $w = u + \frac{\pi}{2}$, $dw = du$.

$$= -2\int_0^{\theta} \log|2\sin(u)|du - 2\int_{\frac{\pi}{2}}^{\theta+\frac{\pi}{2}} \log|2\sin(w)|dw \tag{88}$$

$$= 2\Lambda(\theta) + 2\Lambda\left(\theta + \frac{\pi}{2}\right) - 2\Lambda\left(\frac{\pi}{2}\right) \tag{89}$$

This is almost what we set out to prove, but we have an extra term. Luckily, proposition 7 gives us that

$$\Lambda\left(\frac{\pi}{2}\right) = \Lambda\left(-\frac{\pi}{2}\right) = -\Lambda\left(\frac{\pi}{2}\right), \tag{90}$$

which of course implies that $\Lambda(\frac{\pi}{2}) = 0$, so we are done. □

The reason we are interested in the Lobachevsky function is that we can use it to calculate the volumes of ideal tetrahedra, and thus of hyperbolic knot complements.

Theorem 7. *The volume of an ideal tetrahedron described by edge invariants z_1, z_2, and z_3 is given by $\Lambda(\arg(z_1)) + \Lambda(\arg(z_2)) + \Lambda(\arg(z_3))$.*

For a proof of this fact, see [2]. Now, since we have already found a decomposition of the figure eight knot complement into ideal tetrahedra, let us calculate its volume. Recall that all three edge invariants of both tetrahedra were $\sqrt[3]{-1}$. Since $\arg(\sqrt[3]{-1}) = \arg(e^{\frac{\pi i}{3}}) = \frac{\pi}{3}$, we have that

$$Vol(E) = 2(\Lambda(\frac{\pi}{3}) + \Lambda(\frac{\pi}{3}) + \Lambda(\frac{\pi}{3})) = 6\Lambda(\frac{\pi}{3}). \tag{91}$$

5 Proof of the Volume Conjecture for the Figure Eight Knot

It remains unknown whether the volume conjecture is true for every hyperbolic knot, but it has been proven for several specific knots, including the figure eight knot, depicted in figure 1. We will give a proof due to Ekholm of the conjecture for the figure eight knot, following [3], but with different conventions for q. Habiro and Lê found the following closed formula for every colored Jones polynomial of the figure eight knot (which we will call E):

$$J_N(E;q) = \frac{1}{\{N\}} \sum_{k=0}^{N-1} \frac{\{N+k\}!}{\{N-1-k\}!} \tag{92}$$

where $\{N\} = q^N - q^{-N}$ (see [4] and [5]). However, we want to be able to calculate the limit from conjecture 1, so we want an even more convenient

expression. Expanding the factorial, we see that

$$J_N(E;q) = \frac{1}{\{N\}} \sum_{k=0}^{N-1} \frac{(q^{N+k} - q^{-(N+k)}) \cdots (q - q^{-1})}{(q^{N-k-1} - q^{-(N-k-1)}) \cdots (q - q^{-1})} \tag{93}$$

$$= \frac{1}{\{N\}} \sum_{k=0}^{N-1} (q^{N+k} - q^{-(N+k)}) \cdots (q^{N-k} - q^{-(N-k)}) \tag{94}$$

Now we notice that the middle term of the multiplication is $q^N - q^{-N} = \{N\}$, so

$$J_N(E;q) = \sum_{k=0}^{N-1} \prod_{j=1}^{k} (q^{N+j} - q^{-(N+j)})(q^{N-j} - q^{-(N-j)}). \tag{95}$$

Now if we let $q = e^{\frac{\pi i}{N}}$, we have

$$J_N(E;e^{\frac{\pi i}{N}}) = \sum_{k=0}^{N-1} \prod_{j=1}^{k} (e^{\frac{\pi i(N+j)}{N}} - e^{\frac{-\pi i(N+j)}{N}})(e^{\frac{\pi i(N-j)}{N}} - e^{\frac{-\pi i(N-j)}{N}}) \tag{96}$$

$$= \sum_{k=0}^{N-1} \prod_{j=1}^{k} (e^{2\pi i} - e^{\frac{2\pi ij}{N}} - e^{\frac{-2\pi ij}{N}} + e^{-2\pi i}) \tag{97}$$

$$= \sum_{k=0}^{N-1} \prod_{j=1}^{k} (2 - e^{\frac{2\pi ij}{N}} - e^{\frac{-2\pi ij}{N}}) \tag{98}$$

$$= \sum_{k=0}^{N-1} \prod_{j=1}^{k} 4\sin^2(\frac{\pi j}{N}). \tag{99}$$

Let $f(N;j) := 4\sin^2(\frac{\pi j}{N})$. We can see that $f < 1$ for $0 < j < \frac{N}{6}$ and for $\frac{5N}{6} < j < N$ and that $f > 1$ for $\frac{N}{6} < j < \frac{5N}{6}$, so if we let $g(N;k) := \prod_{j=1}^{k} f(N;j)$, g decreases (as a function of k) when $0 < k < \frac{N}{6}$ and when $\frac{5N}{6} < k < N$ and increases when $\frac{N}{6} < k < \frac{5N}{6}$. Thus g must achieve a maximum at $k = \frac{5N}{6}$, or rather, since N is a positive integer, g achieves a maximum at $k = \lfloor \frac{5N}{6} \rfloor$. There are N terms in the summation $J_N(E;e^{\frac{\pi i}{N}}) = \sum_{k=0}^{N-1} g(N;k)$ and all of them must be positive, so we have

$$J_N(E;e^{\frac{\pi i}{N}}) \leq N g(N; \left\lfloor \frac{5N}{6} \right\rfloor). \tag{100}$$

Note that $g(N; \lfloor \frac{5N}{6} \rfloor)$ must be among the summed terms in $J_N(E;e^{\frac{\pi i}{N}})$, so again since all of the summed terms are positive, we also have

$$g(N; \left\lfloor \frac{5N}{6} \right\rfloor) \leq J_N(E;e^{\frac{\pi i}{N}}). \tag{101}$$

We are closer to being able to calculate $\lim_{N\to\infty} J_N(E; e^{\frac{\pi i}{N}})$ now, but we need to do something about the pesky N that is multiplied by the right hand side of (100) so that we will have the limit of J sandwiched between two equal limits. Since all of the terms in the two inequalities are positive, we will take their logarithms and then divide by N.

$$\frac{\log(g(N; \lfloor \frac{5N}{6} \rfloor))}{N} \leq \frac{\log(J_N(E; e^{\frac{\pi i}{N}}))}{N} \leq \frac{\log(Ng(N; \lfloor \frac{5N}{6} \rfloor))}{N} \tag{102}$$

Now, since $\lim_{N\to\infty} \frac{\log(N)}{N} = 0$, we arrive at

$$\lim_{N\to\infty} \frac{\log(g(N; \lfloor \frac{5N}{6} \rfloor))}{N} \leq \lim_{N\to\infty} \frac{\log(J_N(E; e^{\frac{2\pi i}{N}}))}{N} \leq \lim_{N\to\infty} \frac{\log(g(N; \lfloor \frac{5N}{6} \rfloor))}{N}, \tag{103}$$

which implies

$$\lim_{N\to\infty} \frac{\log(J_N(E; e^{\frac{\pi i}{N}}))}{N} = \lim_{N\to\infty} \frac{\log(g(N; \lfloor \frac{5N}{6} \rfloor))}{N}. \tag{104}$$

Since $g(N,k) = \prod_{j=1}^{k} f(N; j)$,

$$\lim_{N\to\infty} \frac{\log(g(N; \lfloor \frac{5N}{6} \rfloor))}{N} = \lim_{N\to\infty} \frac{\sum_{j=1}^{\lfloor \frac{5N}{6} \rfloor} \log(f(N; j))}{N} \tag{105}$$

$$= \lim_{N\to\infty} \frac{1}{N} \sum_{j=1}^{\lfloor \frac{5N}{6} \rfloor} 2\log(2\sin(\frac{\pi j}{N})) \tag{106}$$

This last expression looks like a right hand rectangular approximation of an integral, so we will finish taking the limit using an integral:

$$= \frac{2}{\pi} \int_0^{\frac{5\pi}{6}} \log(2\sin(x))dx \tag{107}$$

We recognize this integral! We can rewrite this in terms of the Lobachevsky function, so now we have

$$\lim_{N\to\infty} \frac{J_N(E; e^{\frac{\pi i}{N}})}{N} = -\frac{2}{\pi}\Lambda(\frac{5\pi}{6}) \tag{108}$$

Using proposition 7 we have

$$\Lambda(\frac{5\pi}{6}) = \Lambda(\frac{-\pi}{6}) = -\Lambda(\frac{\pi}{6}), \tag{109}$$

and using proposition 8 and proposition 7 again we also have,

$$\Lambda(\frac{\pi}{3}) = 2\Lambda(\frac{\pi}{6}) + 2\Lambda(\frac{2\pi}{3}) = 2\Lambda(\frac{\pi}{6}) - 2\Lambda(\frac{\pi}{3}). \tag{110}$$

Thus we have the identity

$$\Lambda(\frac{5\pi}{6}) = -\frac{3}{2}\Lambda(\frac{\pi}{3}). \tag{111}$$

Going back to the limit from equation 108, we have

$$2\pi \lim_{N\to\infty} \frac{\log|J_N(E; e^{\frac{\pi i}{N}})|}{N} = 6\Lambda(\frac{\pi}{3}) = Vol(E), \tag{112}$$

so we have proven the volume conjecture for the figure eight knot.

References

[1] J. Purcell, "Hyperbolic knot theory." 2010.

[2] J. Milnor, *The Geometry and Topology of Three-Manifolds*, ch. 7, pp. 157–170. Mathematical Sciences Research Institute, 1980.

[3] H. Murakami, "An introduction to the volume conjecture," *arXiv e-prints*, January 2010.

[4] K. Habiro, "On the colored jones polynomial of some simple links (recent progress towards the volume conjecture)," *Surikaisekikenkyusho Kokyuroku*, no. 1172, pp. 34–43, 2000.

[5] T. T. Lê, "Quantum invariants of 3-manifolds: Integrality, splitting, and perturbative expansion," *Topology and its Applications*, vol. 127, no. 1, pp. 125–152, 2003. Proceedings of the Pacific Institute for the Mathematical Sciences workshop "Invariants of Three-Manifolds".